Linköping University Postprint

In-situ surface preparation of nominally on-axis 4H-SiC substrates

J. Hassan, J.P. Bergman, A. Henry and E. Janzén

N.B.: When citing this work, cite the original article.

Original publication:

J. Hassan, J.P. Bergman, A. Henry and E. Janzén, In-situ surface preparation of nominally on-axis 4H-SiC substrates, 2008, Journal of Crystal Growth, (310), 20, 4430-4437.
http://dx.doi.org/10.1016/j.jcrysgro.2008.06.083.
Copyright: Elsevier B.V., http://www.elsevier.com/

Postprint available free at:
Linköping University E-Press: http://urn.kb.se/resolve?urn=urn:nbn:se:liu:diva-15195

In-situ surface preparation of nominally on-axis 4H-SiC substrates

J. Hassan, J.P. Bergman, A. Henry and E. Janzén

[a]Department of Physics, Chemistry and Biology, IFM, Linköping University, S-58183 Linköping, Sweden

Abstract

A study of the in-situ surface preparation has been performed for both Si- and C-face 4H-SiC nominally on-axis samples. The surface was studied after etching under C-rich, Si-rich and under pure hydrogen ambient conditions at the same temperature, pressure and time interval using a hot-wall chemical vapor deposition reactor. The surfaces of all the samples were analyzed using optical microscopy with Normarski diffractional interference contrast and atomic force microscopy with tapping mode before and after in-situ etching. Polishing related damages were found to be removed under all etching conditions, also the surface step structure was uncovered and a few defect-selective etch pits were observed. For the Si-face sample, the best surface morphology was obtained after Si-rich etching conditions with more uniform and small macro-step height which resulted in the lowest surface roughness. For the C-face sample the surface morphology was comparable under all etching conditions and not much difference was found except for the etching rate. Si droplets were not observed under any etching conditions.

Keywords: A1. Atomic force microscopy; A1. Etching; A3. Chemical vapor deposition processes

1. Introduction

SiC is a material suitable for high-power electronic devices that can operate in harsh environment. The material quality, does not yet allow bulk material to be used as voltage supplying layer. Therefore, SiC epitaxy is a key technology for producing device quality layers. Commercially available SiC wafers used for epitaxial growth still have a high density of polishing scratches on the substrate surface [1,2]. High density of structural defects, like micropipes, dislocation clusters and voids, in the substrate produce surface imperfections during polishing and enhance the surface roughness [3]. Generally, both bulk and epitaxial growth are highly dependent on the surface quality of the starting material [4]. The substrate surface damages can affect the epilayer quality by introducing several different kinds of extended defects [5-9].

Random nucleation of 3C polytype inclusions at the substrate–epilayer interface is one of the major problems in the case of epilayer growth on on-axis Si-face 4H-SiC substrate and it has been reported that the substrate surface damages are preferential nucleation sites for these inclusions [10,11]. A high surface roughness of the epilayer grown on on-axis substrate is another problem which could also be related to the morphology of the starting surface. Furthermore, the epitaxial surface roughness values are important in many processing steps in device fabrication, as well as for the performance of many devices.

Therefore, surface preparation prior to the epilayer growth is a crucial step to obtain high-quality smooth homoepitaxial layers. SiC surface preparation is also crucial for the formation of graphene [12, 13], which is a thin layer of carbon formed on the surface after Si out diffuse. The in-situ surface preparation in hydrogen ambient, in the temperature range of 1400–1800 °C, is already known to improve the surface morphology by removing polishing scratches on off-cut substrates [14-18]. In order to avoid the depletion of carbon from the substrate surface through the formation of hydrocarbon, a small amount of propane is used along with the carrier gas during temperature ramp-up which ultimately helps avoiding the formation of Si droplets on the substrate surface and is typically used as a routine in-situ surface preparation method [19]. An effect of adding propane to the hydrogen flow is also a slightly decreased etch rate and a smoother surface. Normal temperature used for epitaxial growth is around 1600 °C and the best etching results are reported at a temperature of 1400 °C [20]. With induction heating system it takes 5–10 min to reach from 1400 °C to a stable growth temperature of 1600 °C. During temperature ramp-up, the surface etching is inevitable and can effectively change the surface morphology. Therefore, it is important to know how the surface looks like prior to the start of the epilayer growth.

In-situ surface preparation under C-rich conditions (H_2+C_3H_8) has been reported for both off- and on-axis substrates; etching under pure hydrogen conditions was shown to produce high density of Si droplets on the surface of off-cut substrates [21]. The in-situ surface preparation of 8° and 4° off-cut substrate, under Si-rich conditions, has also been shown to improve the surface morphology [22]. The in-situ surface preparation under different ambient conditions may have different effect on the on-axis substrates. We report here the experimental results of the in-situ surface preparation of both Si- and C-face on-axis samples under C-rich conditions (H_2+C_3H_8), Si-rich conditions (H_2+SiH_4) and in pure hydrogen ambient.

2. Experimental procedure

For the etching study two commercially obtained nominally on-axis 2″ 4H-SiC wafers, one with Si-face [0 0 0 1] polished and one with C-face $[0\ 0\ 0\ \bar{1}]$ polished, were cut into small 1 cm^2 pieces. All samples were cleaned using standard wafer cleaning process. A horizontal hot-wall CVD reactor [23] was used for the in-situ etching of the samples. Hydrogen purified through heated palladium membrane was used as carrier gas. Etching was performed on both Si- and C-face polished sample under C-rich, Si-rich and in pure hydrogen ambient conditions. During C- and Si-rich conditions the flow rates of C_3H_8 and SiH_4, added to the 57 l/min flow rate of hydrogen, were 25% and 20% of the flow rates normally used for SiC growth, respectively. The counting of the etching time was started from a temperature of 1530 °C. All etching experiments were performed for 20 min each at a temperature of 1580 °C and a pressure of 200 mbar. Optical microscopy with Nomarski interference contrast and atomic force microscopy (AFM) in tapping mode were used to observe the surface morphology, step structure and surface roughness on all samples before and after etching.

3. Results and discussion

Optical images taken from as-received samples, from Si- and C-faces, are shown in Fig. 1a and b, respectively. Along with the polishing scratches, small pin-hole like depressions marked with circles can also be seen in both images. AFM performed on both faces revealed two different kinds of features on the surface, independent of the surface orientation:

(i) shallow and deep polishing scratches,

(ii) shallow and deep depressions.

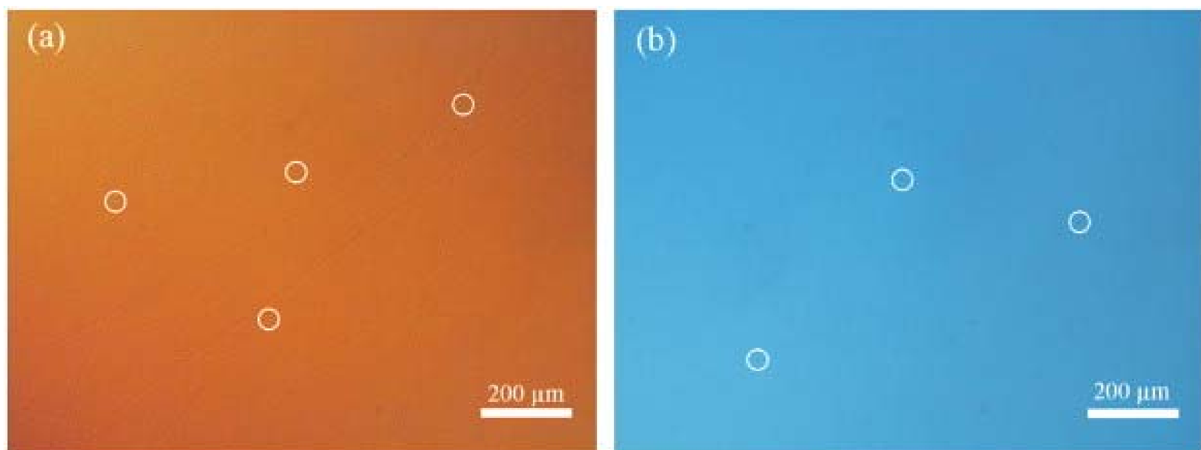

Fig. 1. Optical image taken from as-received (a) Si face and (b) C face. In both images the pin-holes are highlighted with circles.

The depth of the shallow polishing scratches as measured through section analysis of the AFM image (Fig. 2a) is ~3 nm, while for deep polishing scratches it is ~10 nm. Figs 2b and c are high-magnification images taken from the depressions marked with arrows in Fig. 2a. These features were identified as small pin-hole like depressions with optical microscopy. The section analysis of these micrographs shows that the diameters of the depressions are ~ 267 and ~343 nm while the depth is ~3.1 and ~15.9 nm, respectively. These depressions could also be related to the polishing process.

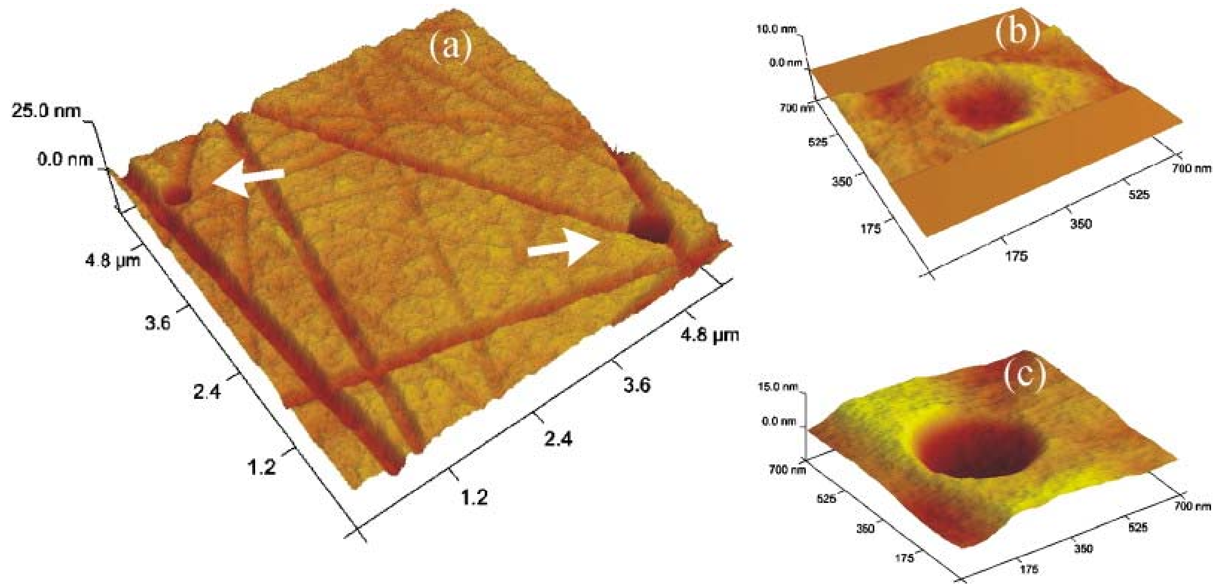

Fig. 2. (a) 5×5 µm^2 AFM scan taken from the Si-face sample. Scratches from polishing and two depressions, marked with arrows, are observed (b) high magnification image taken from small diameter depression and (c) high magnification image taken from large diameter depression.

3.1. Etching under C-rich conditions

Optical images taken from the Si-face polished sample after etching under C-rich conditions (Fig. 3a) show heavy step bunching, which results in the formation of macro-steps and very wide terraces on the surface. The macro-steps are neither straight, nor continuous. A few randomly distributed round etch pits also appeared on the surface after etching. The density of such pits is found to be $\sim$300 cm^{-2} which is too low to be attributed to the normal screw dislocations density (~3×10^3 cm^{-3}) in commercially available 4H-SiC substrates [24]. On the other hand, optical micrographs (Fig. 3b) taken from C-face sample etched under the same conditions show a mirror-like surface without any defects related etch pits. This could be related to the lower surface energy on C-face compared to on Si-face [25]. The high surface energy on Si-face is lowered through the mechanism of step bunching. The polishing scratches and deep depressions in the scratched lines present on the surface of as-received samples vanished after etching.

In order to examine the surface roughness and surface step structure AFM in tapping mode was performed. A wide area scan of 100×100 µm^2 taken from the Si-face sample (Fig. 4a) shows a surface roughness (RMS) of 17 nm. The macro-step height is between 60 and 90 nm and the terrace width is between 20 and 40 µm. The macro-steps are clearly not continuous. Along with these macro-steps, the in-situ etching uncovered three different kinds of features on the surface:

(i) shallow etch pits,

(ii) periodic train of micro-steps,

(iii) deep round etch pits.

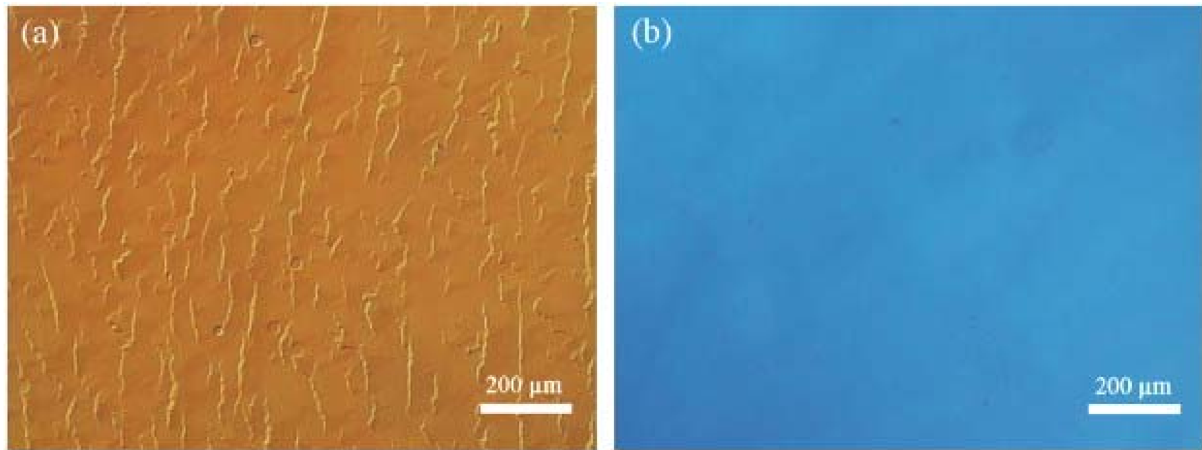

Fig. 3. Optical image taken from (a) Si-face and (b) C-face sample etched in C-rich conditions.

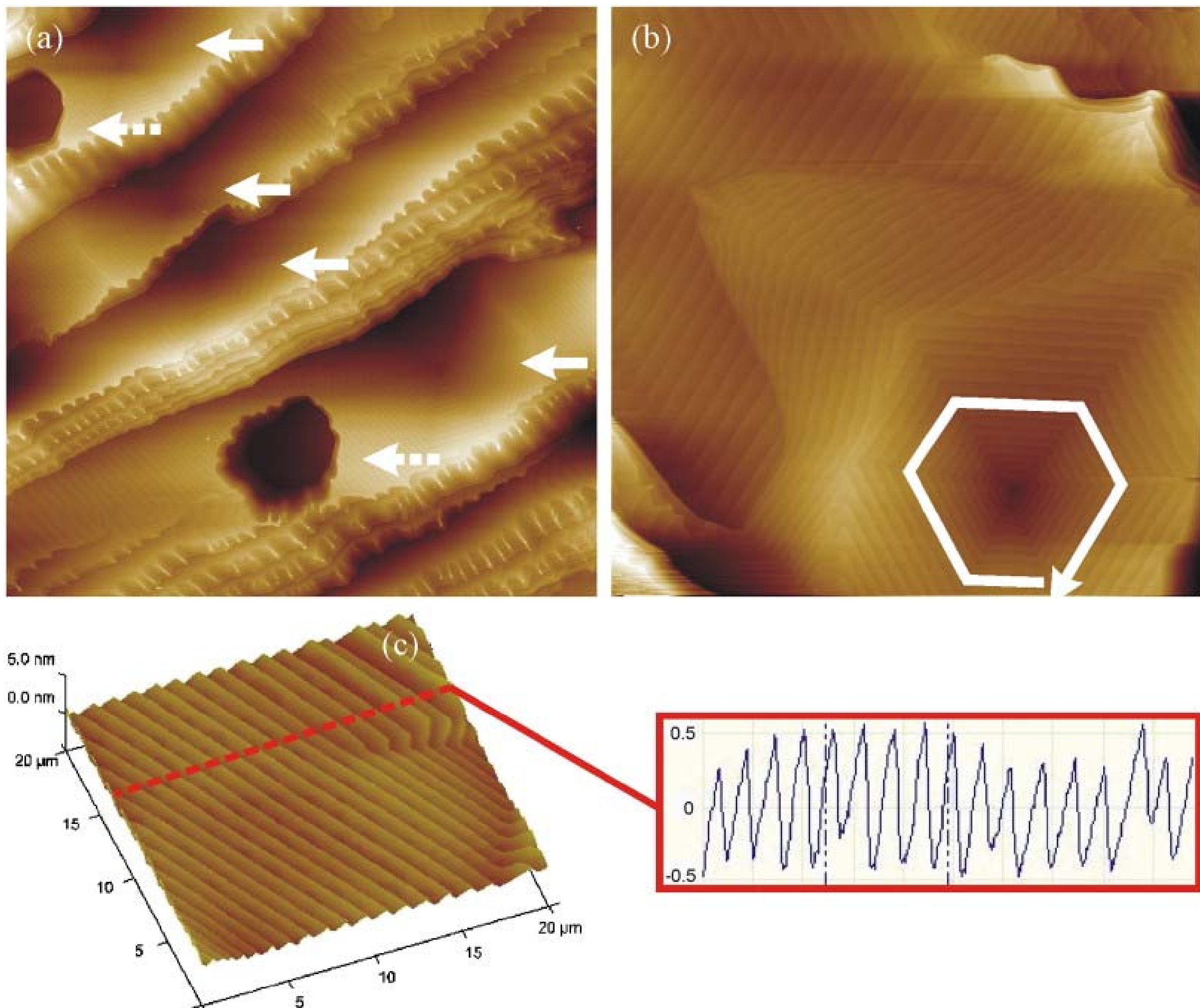

Fig. 4. (a) AFM image 100×100 μm^2 of Si-face etched in C-rich conditions. Macro-steps are visible. (b) 50×50 μm^2 scan taken around shallow hexagonal etch pit and (c) high-resolution 20×20 μm^2 scan taken from wide terrace, far away from the center of shallow hexagonal etch pit, showing micro-steps of half of unit cell height for 4H-SiC.

3.1.1. Shallow etch pits

On wide terraces a high density of shallow etch pits with hexagonal spiral-like structure were observed in AFM surface topograph and are marked with solid arrows in Fig. 4a. Analysis of the whole sample surface with AFM showed that such shallow etch pits are present over the entire sample surface and that their density is comparable to that of elementary screw dislocation's density in 4H-SiC. High-resolution scans around these shallow etch pits reveal a spiral-like feature (Fig. 4b) with micro-step height of 2–4 bilayers of 4H-SiC. Etching, in many ways, is a reverse process to the crystal growth. Similar to the crystal growth in layer-by-layer fashion at certain supersaturation, etching could be performed at certain undersaturation and the layer height observed on the etched surface may be the height of a single-crystal cell. Screw dislocations intersecting the surface provide growth steps on the surface and are responsible for growth below a critical supersaturation [26]. During growth the step advances and rotates in the form of a spiral and appears as a hillock on the surface. Similarly, in the case of etching, screw dislocations intersecting the surface provide steps which rotate in the form of spirals in opposite direction and will appear in the form of etch pits on the surface. Therefore, shallow etch pits appearing on the surface with hexagonal spiral-like feature are attributed to screw dislocations intersecting the surface normally. The step height corresponds to the magnitude and the clockwise or anti-clockwise rotation of the spiral gives the sense of the direction of Burger vector. Therefore, hexagonal spiral-like structure in Fig. 4b corresponds to a screw dislocation with a Burger vector of −1c as the step height is 1 nm which corresponds to unit cell height in 4H-SiC and the spiral is moving clockwise towards the reader [27].

The depth of such shallow pits varies a few nm over the entire sample surface. In Fig. 4b, the depth of the etch pit measured from the surface is about 12 nm. The steps at the interfaces of all six facets of the hexagon are intercepting at the facet boundary. In some cases, the step height is 2 bilayers on each facet which indicate that the unit cell steps dissociate into two steps with half unit cell height. Shallow pits are associated with low etch rate whereas deeper pits with higher local etch rate. The local etch rate may depend on three factors: (i) local thermodynamic conditions over the sample surface like temperature, pressure and concentration of C and Si containing species in the gas phase (ii) local doping of the substrate and (iii) local orientation of the surface planes or angle of the dislocation line relative to the surface. In our case local orientation of the surface planes is probably the main reason for different local etching rates, resulting in different depth of the etch pits.

3.1.2. Periodic train of micro-steps

The micro-steps originating from elementary screw dislocations spread over the entire sample surface. Far away from the core of screw dislocation, the micro-steps appeared in the form of a periodic and linear train of micro-steps with step height of 2–4 bilayers as shown in Fig. 4c. There was no evidence of step bunching on the steps originating from screw dislocations either inside or outside of the shallow etch pits.

3.1.3. Deep round etch pits

The deep round etch pits marked with broken arrows in Fig. 4a were identified to be the same as seen in the optical image (Fig. 3a). High magnification AFM images revealed two different structures of these pits. The first one showed steep walls and a hexagonal hole in the middle of the bottom of the etch pit as shown in Fig. 5a. A high-magnification image taken from the

etch pit is shown in the inset of Fig. 5a. The bottom is convex shaped and covered with micro-steps of unit cell height. A hexagonal hole appeared in the middle of the bottom. The hexagonal hole is too deep for the AFM tip to reach its bottom. The diameter of the inner hexagonal hole is between 1 and 2 µm, the diameter of outer etch pit is between 6 and 8 µm while the height of the steep wall is ~15 nm. The multiple steps of unit cell height originating from the hexagonal hole indicate that it is probably a micropipe with large *c* Burger vector. The second kind of deep etch pit appeared with less steep walls and a flat bottom, as shown in Fig. 5b. A high-magnification image taken around the etch pit, shown in the upper inset in Fig. 5b, revealed that the side walls are composed of micro-steps with very small terrace width, but still the side walls are inclined with respect to the bottom of the etch pit. In this case there was no hexagonal hole observed in the middle of the bottom. The shape of the bottom is convex with the center of the spiral higher than the rest of the bottom area. The diameter of outer edges of the etch pit is between 15 and 25 µm while the depth is ~10 nm. A high magnification image taken from the bottom of the etch pit, shown in the lower inset in Fig. 5b, revealed that it is covered with micro-steps of unit cell height indicating that these steps are originating from an elementary screw dislocation.

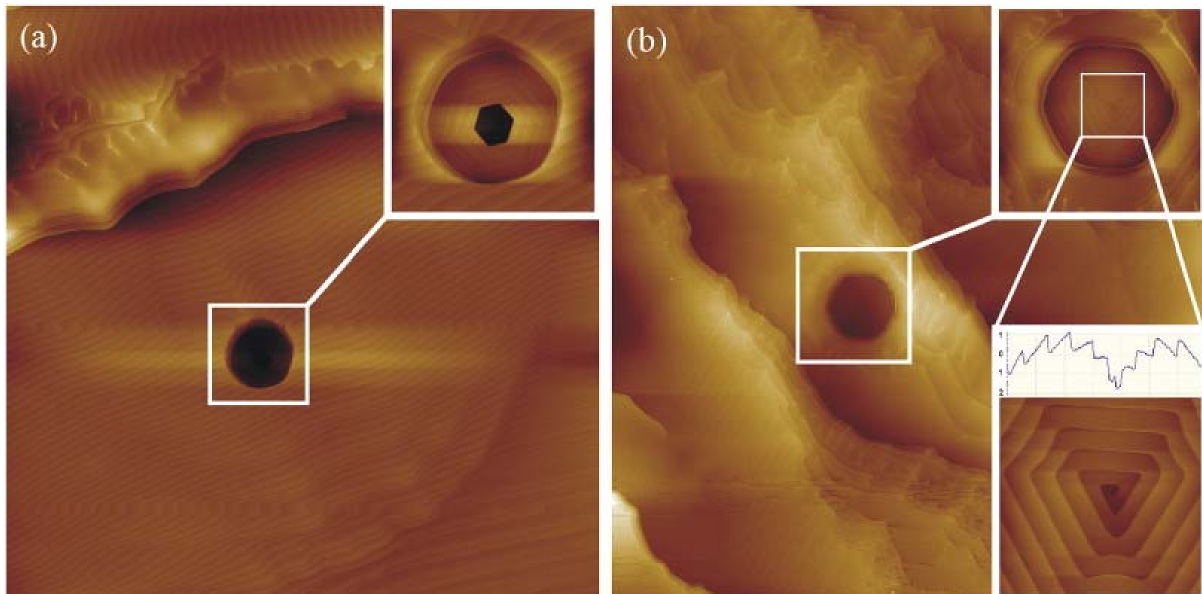

Fig. 5. AFM image taken from Si-face sample etched in C-rich conditions (a) 50×50 µm^2 area scan, the inset is a 10×10 µm^2 scan taken from the area marked with white square (b) 100×100 µm^2 area scan, the top inset is a 20×20 µm^2 scan taken from the area marked with white square while the bottom inset is a 8×8 µm^2 AFM scan taken at the bottom of the etch pit, elementary screw dislocation related spiral with unit cell step height is seen.

A 20×20 µm^2 surface topographic scan taken from the C-face substrates etched under the same conditions is shown in Fig. 6. The surface consists of very regular and periodic micro-steps. The step height is equal to one bilayer i.e. 2.5 Å. A wavy pattern perpendicular to the steps is observed all over the sample. No step bunching or etch pits similar to the Si-face are seen on the C-face sample.

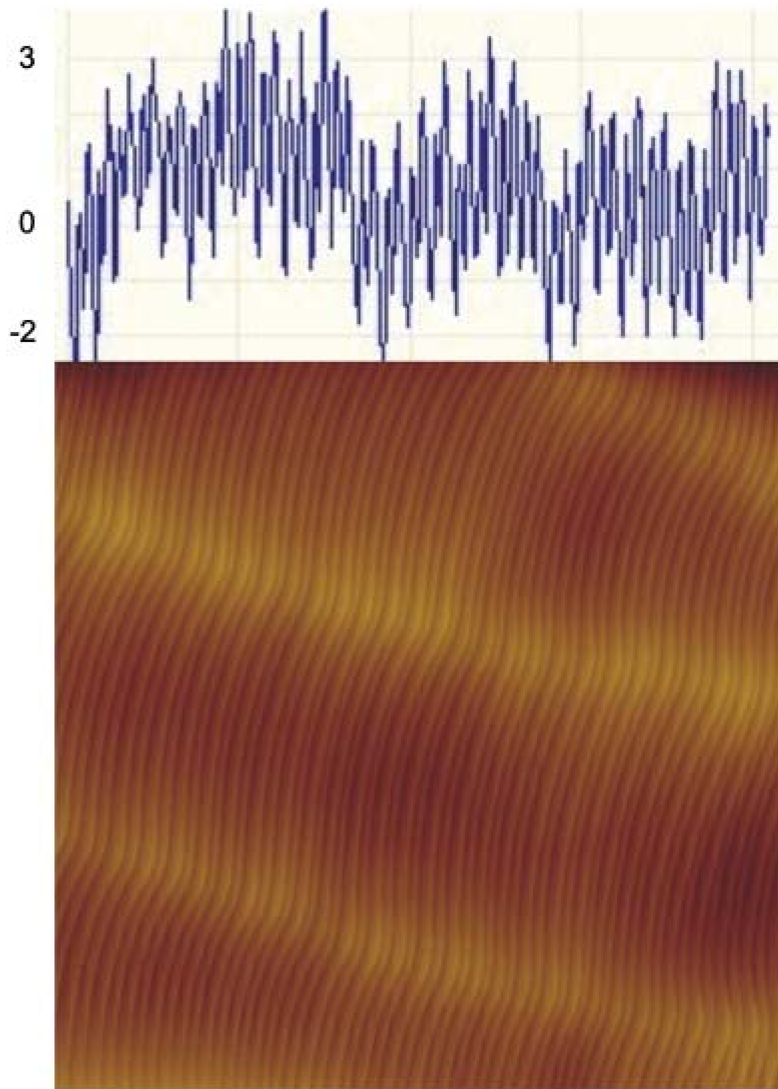

Fig. 6. 20×20 μm² AFM image taken from the C-face sample etched in C-rich conditions. The scale on the top is in nm.

3.2. Etching under Si-rich conditions

Optical images taken from the Si-face sample after etching in Si-rich conditions also showed macro-step bunching but the macro-steps are straight, periodic and continuous resulting in evenly distributed wide terraces, as seen in Fig. 7. The density of deep etch pits on the surface was found to be similar to the Si-face etched surface in C-rich conditions.

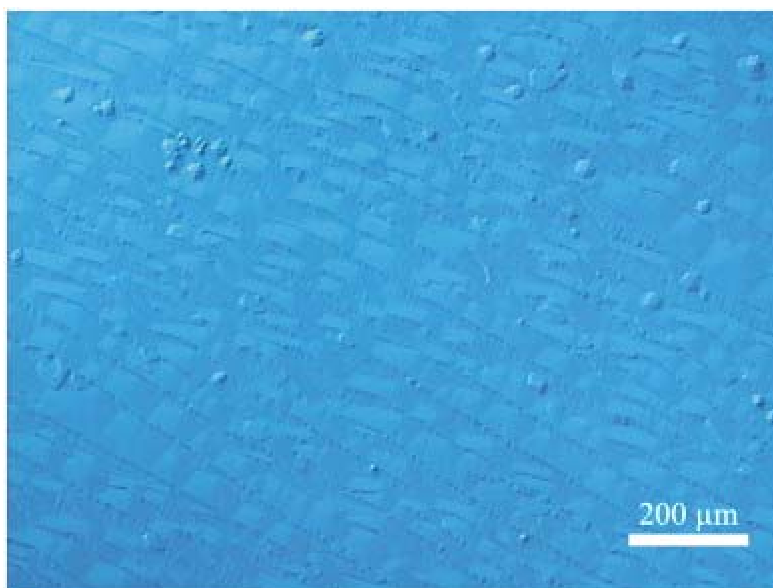

Fig. 7. Optical image taken from the Si-face sample etched in Si-rich conditions.

Optical micrographs taken from the C-face sample after etching show mirror-like surface. Neither macro-steps nor etch pits are seen. All kinds of polishing related surface damages are removed after etching.

A wide area AFM scan (100×100 μm^2, Fig. 8a) of an etched Si-face has a surface roughness (RMS) of 6 nm which is 3 times less than the surface roughness as measured on the Si-face sample etched in C-rich conditions at the same temperature, pressure and time interval. The macro-step height is 15–20 nm and terrace width is 30–40 μm. The smaller surface roughness, compared to that on the Si-face sample etched in C-rich conditions, is due to smaller and more even distribution of macro-steps. In-situ etching under Si-rich conditions also resulted in similar kind of features on the surface as discussed in the previous case for Si-face sample etched in C-rich conditions, but in this case the height of micro-steps produced by elementary screw dislocations is always equal to unit cell height of 4H-SiC while the terrace width is about 135 nm. High-resolution image taken from wide terrace, given in the inset in Fig. 8a, shows a straight periodic train of micro-steps of unit cell height. A typical AFM scan containing both shallow and deep pits is given in Fig. 8b. The deep etch pits show similar kind of morphology as observed in the case of Si-face etched in C-rich conditions. A high magnification AFM scan taken around a shallow etch pit is shown in the inset in Fig. 8b where unit cell height micro-steps with anti-clock wise rotation of spiral correspond to a threading screw dislocation with 1c Burger vector.

AFM scans taken from C-face polished substrates etched in Si-rich conditions show similar kind of features as seen in the case of C-face etched in C-rich conditions.

3.3. Etching in pure hydrogen

The surfaces etched under Si- or C-rich conditions were finally compared to the surfaces etched with pure hydrogen. Optical image taken from the Si-face sample etched in pure hydrogen (Fig. 9a) shows heavy step-bunching. The step density is higher as compared to the

Si-face sample etched in either Si- or C-rich conditions but the steps appeared with non-periodic zig-zag shape structure. Defect-selective deep etch pits appeared in a large number ~3000 cm^{-2} and are comparable to the screw dislocation density in commercially available 4H-SiC substrates. This shows that almost all of the screw dislocations selectively etched in pure hydrogen ambient. Even though the susceptor was coated with SiC but due to the ageing of the susceptor, graphite can be exposed and under pure hydrogen conditions the atmosphere inside the susceptor could be a little biased with C containing species. C-face sample does not show any features in optical image but only a mirror-like surface.

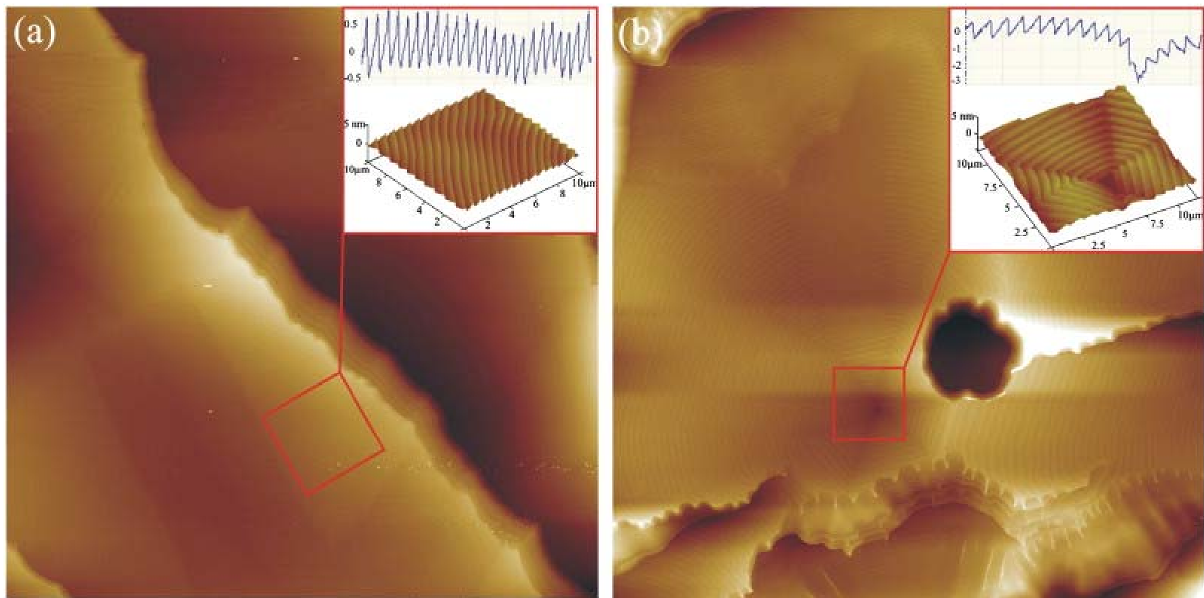

Fig. 8. AFM images taken from Si-face etched sample in Si-rich conditions (a) 100×100 μm^2 area scan showing macro-steps, the inset is a 10×10 μm^2 area scan taken from the wide terrace showing micro-steps and (b) 80×80 μm^2 area scan showing both shallow and deep etch pits, the inset is a 12×12 μm^2 area scan taken around a shallow etch pit.

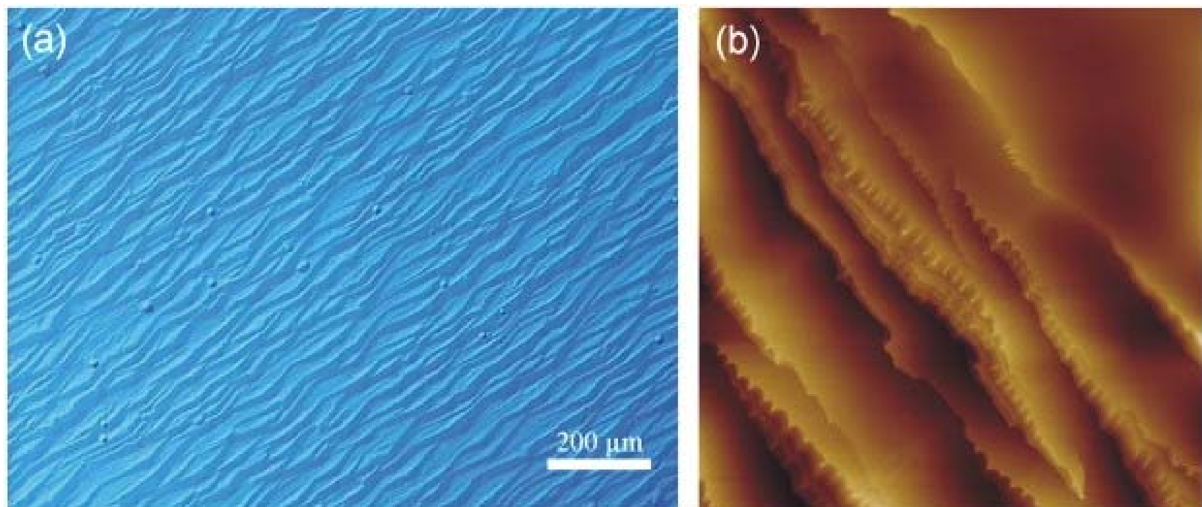

Fig. 9. (a) Optical image taken from Si-face etched in pure hydrogen. (b) AFM image (100×100 μm^2) of Si-face sample etched in pure hydrogen. Macro-steps are visible.

AFM studies on this sample showed similar kind of features as that for the Si-face sample etched either in Si- or C-rich conditions. A wide area AFM scan of 100×100 μm^2 (Fig. 9b)

shows a surface roughness of 10.7 nm. The macro-step height is varying between 30 and 40 nm and the terrace width is between 20 and 30 µm. A closer look at the wide terrace surface reveals that it is covered with micro-steps generated by elementary screw dislocation with step height of 2–4 bilayers while the terrace width is 130–150 nm. The surface morphology of the C-face sample, as revealed by AFM was similar to the previous cases. In-situ etching under pure hydrogen ambient was also found to remove all polishing related surface damages; no Si droplets were observed on the surface.

3.4. Etching rate

In order to measure the etch rate 6 and 9-µm thick epilayers were grown on both Si- and C-face substrates, respectively. The layer thickness and per consequence the growth rate were higher on the C-face sample than on the Si-face sample, probably due to the higher step density. Etching was performed on both Si- and C-face grown epilayers simultaneously for each etching condition. The etch rate was estimated through measuring epi thickness before and after etching with Fourier transform infrared reflectance spectroscopy (FTIR). If we only consider the bonding structure we would expect similar etching rates for both faces in pure hydrogen ambient. For the etching rate on the Si-face etched under Si-rich conditions we might instead expect a higher etch rate if a thin liquid Si film exists on the surface. The interfacial surface free energy between a solid and a liquid is lower than the interfacial surface free energy between a solid and a vapor. Therefore, under Si-rich conditions we would expect that the environment above the surface is more like interface between a solid and a liquid. Hence, a lower effective C/Si ratio on the surface lowers the surface free energy [28] and changes the etching mechanism. C-rich conditions, on the other hand, do not change the surface free energy as C does not melt. Nevertheless, experimentally we found that the difference of the etching rate was very small on Si-face sample under all etching conditions, indicating that the surface etching on Si-face under these conditions is mainly controlled by the thermal decomposition of the surface Si–C bilayer due to high temperature. On the C-face sample, however, the surface etch rate was higher in Si-rich conditions as compared to that in pure hydrogen or C-rich conditions.

A comparison of the surface roughnesses (RMS), macro-step height, micro-step height and etching rates for both Si- and C-face etched under different ambient at same temperature, pressure and time interval is given in Table 1. On Si-face samples etched under Si-rich conditions the macro-step height is smaller and a low surface roughness is observed, also the micro-step height is always equal to unit cell height.

4. Conclusions

In-situ etching in both Si- and C-rich conditions removes the polishing related surface scratches and reveals the surface atomic steps. The Si-face shows macro-step bunching while the C-face shows continuous and periodic micro-steps without any step bunching for all three etching conditions. The Si-face after etching in Si-rich conditions shows more linear, periodic, continuous and evenly distributed macro-steps. Also, the surface roughness of the Si-face sample etched under Si-rich conditions is 3 times smaller than after etching in pure hydrogen or C-rich conditions. Steps originating from the elementary screw dislocations on the Si-face sample etched in Si-rich conditions are always of unit cell height. Therefore, Si-rich conditions can be effectively used to prepare nominally on-axis Si-face sample before homoepitaxial growth. Si droplets were not observed under any of the etching conditions. For

Si-face the etch rate was found to be almost the same under all etching conditions but on C-face etching was found to be higher under Si-rich conditions.

Table 1: Macro-step height, micro-step height, surface roughness and etch rate on both Si- and C-face samples under C-rich, Si-rich and pure hydrogen ambient conditions

Face	C-rich conditions	Si-rich conditions	Pure hydrogen
Macro-step height (nm)			
Si	60–90	15–20	30–40
C	0	0	0
Micro-step height (nm)			
Si	0.5–1	1	0.5–1
C	2.5	2.5	2.5
Surface roughness (RMS) nm			
Si	17	6	10.7
C	0.330	0.296	0.31
Etch rate (μm/h)			
Si	2.26	2.34	2.23
C	1.68	2.24	1.34

Acknowledgments

The authors are grateful for the financial support from Norstel AB, Swedish Governmental Agency for Innovation Systems, (Vinnova), and Swedish Energy Agency (STEM).

References

1 C.H. Li, R.J. Wang, J. Seiler and I. Bhat, *Mater. Sci. Forum* **457–460** (2004), p. 801.
2 W. Qian, M. Skowronski, G. Augustine, R.C. Glass, D. Hobgood and R.H. Hopkins, *J. Elec. Chem. Soc.* **142** (1995), p. 4290.
3 R.T. Bondokov, T. Lashkov and T.S. Sudarshan, *Jpn. J. Appl. Phys.* **43** (2004), p. 43.
4 R.C. Glass, D. Henshall, V.F. Tsvetkov and C.H. Carter, *J. Mater. Res. Bull.* (1997), p. 30.
5 A. Ellison, J. Zhang, J. Peterson, A. Henry, Q. Wahab, J.P. Bergman, Y.N. Makarov, A. Vorob'ev, A. Vehanen and E. Janzen, *Mater. Sci. Eng. B* **61–62** (1999), p. 113.
6 J.A. Powell, D.J. Larkin, L. Zhou and P. Pirouz, in: Transactions of the Third International High Temperature Electronics Conference, Sandia National Laboratories, Albuquerque (1996) p. II-3.
7 J.A. Powell and D.J. Larkin, *Phys. Stat. Sol. B* **202** (1997), p. 529.
[8] J. Hassan, J.P. Bergman, A. Henry, E. Janzén, J. Appl. Phys., submitted for publication.
9 L. Zhou, V. Audurier, P. Pirouz and J.A. Powell, *J. Electrochem. Soc.* **144** (1997), p. L161.

10 S. Nakamura, T. Kimoto and H. Matsunami, *J. Crystal Growth* **256** (2003), p. 341.
11 J. Hassan, J.P. Bergman, A. Henry and E. Janzén, *Mater. Sci. Forum* **556–557** (2007), p. 53.
12 C. Berger, Z. Song, T. Li, X. Li, A.Y. Ogbazghi, R. Feng, Z. Dai, A.N. Marchenkov, E.H. Conrad, P.N. First and W.A. de Heer, *J. Phys. Chem. B* **108** (2004), p. 19912.
13 A.J. van Bommel, J.E. Crombeen and A. van Tooren, *Surf. Sci.* **48** (1975), p. 463.
14 C. Hallin, F. Owman, P. Mårtensson, A. Ellison, A. Konstantinov, O. Kordina and E. Janzén, *J. Crystal Growth* **181** (1997), p. 241.
15 V. Ramachandran, M. Brady, A. Smith, R. Feenstra and D. Greve, *J. Electron. Mater.* **27** (1998), p. 308.
16 A. Kawasuso, K. Kojima, M. Yoshikawa, H. Itoh and K. Narumi, *Appl. Phys. Lett.* **76** (2000), p. 1119.
17 P. Martensson, F. Owman and L.I. Johansson, *Phys. Stat. Sol. B* **202** (1997), p. 501.
18 S. Dogan, A. Teke, D. Huang, H. Morkoç, C.B. Roberts, J. Parish, B. Ganguly, M. Smith, R.E. Myers and S.E. Saddow, *Appl. Phys. Lett.* **82** (2003), p. 3107.
19 A.A. Burk, L.B. Rowland, G. Augustine, H.M. Hobgood and R.H. Hopkins, *in: III-Nitride, SiC and Diamond Materials for Electronic Devices Symposium* (1996), p. 275.
20 S. Soubatch, S.E. Saddow, S.P. Rao, W.Y. Lee, M. Konuma and U. Starke, *Mater. Sci. Forum* **483–485** (2005), p. 761.
21 C. Hallin, F. Owman, P. Mårtensson, A. Ellison, A. Konstantinov, O. Kordina and E. Janzén, *J. Crystal Growth* **181** (1997), p. 241.
22 K. Kojima, S. Kuroda, H. Okumura and K. Arai, *Mater. Sci. Forum* **556–557** (2007), p. 85.
23 A. Henry, J. ul Hassan, J.P. Bergman, C. Hallin and E. Janzén, *Chem. Vapor Deposition* **12** (2006), p. 475.
24 A.R. Powell, R.T. Leonard, M.F. Brady, St.G. Müller, V.F. Tsvetkov, R. Trussell, J.J. Sumakeris, H. McD. Hobgood, A.A. Burk, R.C. Glass and C.H. Carter, *Mater. Sci. Forum* **457–460** (2004), p. 41.
25 T. Kimoto, A. Itoh and H. Matsunami, *Appl. Phys. Lett.* **66** (1995), p. 3645.
26 W.K. Burton, N. Cabrera and F.C. Frank, *Nature* **163** (1949), p. 398.
27 X. Ma, *J. Appl. Phys.* **99** (2006), p. 063513.
28 K. Kojima, S. Nishizawa, S. Kuroda, H. Okumura and K. Arai, *J. Crystal Growth* **275** (2005), p. e549.